

Process Development for the Enzymatic Gram-Scale Production of the Unnatural Nucleotide Sugar UDP-6-Azido-GalNAc

Hannes Frohnmeyer,^[a] Jorge M. M. Verkade,^[b] Markus Spiertz,^[c] Andreas Rentsch,^[d] Niels Hoffmann,^[a] Milan Sobota,^[c] Frank Schwede,^[d] Peter Tjeerdsma,^[b] and Lothar Elling^{*[a]}

Azido sugars hold great promise as substrates in numerous click-chemistry applications. However, the synthesis of activated azido sugars is limited by cost and complexity. Conventional chemical activation methods are intricate and time-consuming. In response, we have developed a process for the large-scale production of UDP-6-azido-GalNAc through enzymatic nucleotide sugar synthesis on a gram scale. Our optimization strategies encompassed refining the process parameters of an enzyme cascade featuring NahK from *Bifidobacterium longum* and AGX1 from *Homo sapiens*. Using the repetitive-batch-mode technology, we synthesized up to 2.1 g of UDP-6-azido-GalNAc, achieving yields up to 97% in five consecutive batch cycles

using a single enzyme batch. The synthesis process demonstrated to have total turnover numbers (TTNs) between 4.4–4.8 g of product per gram of enzyme (g_p/g_E) and STYs ranging from 1.7–2.4 g per liter per hour ($g^*L^{-1}h^{-1}$). By purification of a product solution pool containing 2.6 g (4.1 mmol) UDP-6-azido-GalNAc, 2.1 g (2,122.1 mg) UDP-6-azido-GalNAc (sodium salt) with a purity of 99.96% (HPLC) were obtained. The overall recovery after purification was 81% (3.32 mmol). Our work establishes a robust production platform for the gram-scale synthesis of unnatural nucleotide sugars, opening new avenues for applications in glycan engineering.

Introduction

The successful azido/alkyne derivatization of sugars in combination with “click chemistry” represents a new leap in the field of bioconjugates. In recognition of this pioneering work, the Nobel Prize in Chemistry was awarded to Carolyn R. Bertozzi, Morten Meldal, and K. Barry Sharpless in 2022.^[1] Click chemistry has become indispensable for bio-orthogonal labeling, protein glycosylation, pharmaceutical applications, or biomaterial sciences. The use of azido/alkyne-derivatized sugars for *in vivo* labeling surface glycoproteins has been successfully demon-

strated in several studies.^[2] For example, specific glycan installation sites were identified through bioorthogonal reactions, particularly the Staudinger ligation, providing a more comprehensive understanding of glycan metabolism in cells and organisms.^[3–7] Implementing strain-promoted azide-alkyne cycloaddition (SPAAC) by the Bertozzi group enabled the use of copper-free click chemistry in biological systems. This technology enabled the precise characterization of glycosylated biomolecules and their synthetic pathways and is now utilized to develop the latest generation of highly specific antibody-drug conjugates (ADCs).^[8]

Therefore, establishing suitable glycoengineering methods is pivotal in advancing the technology for developing ADCs.^[9] Specifically, azido-derivatized nucleotide sugars were strategically used with copper-free click chemistry to modify the N-glycan core structure of IgGs, as demonstrated with 9-azido-Neu5Ac.^[10] This innovative approach marks a significant milestone in creating novel and powerful ADCs. An illustrative example of N-glycan remodelling is exemplified by the GlycoConnect™ technology to generate stable and homogeneous ADCs.^[11–12] This process involves the selective trimming of N-glycans to a single *N*-acetylglucosamine (GlcNAc) residue, followed by introducing 2-azido or 6-azido-*N*-acetylgalactosamine. The functionalization of mAbs enables the precise conjugation of various potent drug payloads by copper-free click chemistry, leading to a consistent and tailored assembly of drug-conjugated antibodies.^[11–12]

For the production of nucleotide sugar used in the synthesis of derivatized ADCs, both chemical and chemoenzymatic synthesis methods are accessible, whereby chemical synthesis of nucleotide sugars includes several protecting and deprotecting

[a] H. Frohnmeyer, N. Hoffmann, Prof. Dr. L. Elling
RWTH Aachen University
Laboratory for Biomaterials, Institute of Biotechnology and Helmholtz-Institute for Biomedical Engineering
Pauwelsstraße 20, 52074 Aachen, Germany
+49-241-80-28350
E-mail: l.elling@biotec.rwth-aachen.de

[b] Dr. J. M. M. Verkade, P. Tjeerdsma
Synaffix BV
Pivot Park, Kloosterstraat 9, 5349 AB, Oss, The Netherlands

[c] M. Spiertz, M. Sobota
SeSaM-Biotech GmbH
Forckenbeckstraße 50, 52074 Aachen, Germany

[d] Dr. A. Rentsch, Dr. F. Schwede
Biolog Life Science Institute GmbH & Co. KG
Flughafendamm 9a, 28199 Bremen, Germany

Supporting information for this article is available on the WWW under <https://doi.org/10.1002/cssc.202400311>

© 2024 The Authors. ChemSusChem published by Wiley-VCH GmbH. This is an open access article under the terms of the Creative Commons Attribution License, which permits use, distribution and reproduction in any medium, provided the original work is properly cited.

steps.^[13] A widespread chemical method is the MacDonald reaction, which allows α -phosphorylation of the C1 position of anomeric acetylated sugar using phosphoric acid.^[14] The MacDonald reaction has also been used for the C1 phosphorylation of sugars with azido and alkyne motifs, showing that both motifs remain stable even under harsh reaction conditions.^[15] A further common method for the formation of a nucleotide sugar is the Koharna method which involves the formation of phosphoromorpholidate using *N, N'*-dicyclohexylcarbodiimide and DMSO.^[16] Through chemical synthesis, rare and unnatural sugars can be readily formed, as exemplified by the efficient synthesis of the 6-azido-derivatized nucleotide sugar UDP-6-azido-GalNAc. This compound was recently synthesized in a 12 g scale within a span of two days.^[11] However, chemical synthesis often has low yields for sugar 1-phosphates, and α and β conformers are present at varying rates.^[14] In this context, only α conformers are usable for sugar activation resulting in a reduced product yield for the chemical synthesis. In contrast, the stereospecificity of sugar kinases can be exploited to form C1- α phosphorylated monosaccharides in high yields.^[17] *N*-acetyl hexosamine kinase from *Bifidobacterium longum* (*B/NahK*) is particularly interesting for the anomeric α -phosphorylation of derivatized hexosamine-sugars. Several studies have shown that NahK exhibits a noteworthy ability to phosphorylate GlcNAc and GalNAc derivatives at the C1 position.^[17–19] This promiscuity was notably demonstrated with 6-azido, 6-thio, and 6-fluoro GlcNAc, elevating the yields from 20% in chemical synthesis to 84%.^[18] Additionally, for the synthesis of a nucleotide activated sugar, *B/NahK* is often used in combination with UDP-*N*-acetylgalactosamine diphosphorylase from *Homo sapiens* (*HsAGX1*). This enzyme cascade is especially robust for the production of UDP-*N*-acetylglucosamine (UDP-GlcNAc) and UDP-*N*-acetyl-galactosamine (UDP-GalNAc).^[20–21] Furthermore, several nucleotide sugar derivatives such as UDP-6-azido-*N*-acetylgalactosamine (UDP-6-azido-GalNAc) or UDP-6-azido-GlcNAc were synthesized by this cascade.^[22–23]

However, establishing an efficient synthetic enzyme cascade poses significant challenges.^[24–25] In recent years, diverse enzyme-based production processes for nucleotide sugars have emerged.^[13,24–32] This progress has paved the way for the large-scale production of nucleotide sugars through repetitive utilization of enzymes, resulting in maximized product output in the synthesis process.^[21] Notably, using this repetitive batch (rep.-batch) procedure yielded valuable nucleotide sugars at multi-gram scales.^[20,25] With the establishment of enzymatic production protocols for essential nucleotide sugars, the pursuit of producing nucleotide sugar derivatives, such as UDP-6-azido-GalNAc, has gained significant interest. Existing enzyme cascades are primarily described for production at the milligram scale or involve multi-step protocols necessitating one or more purification steps.^[33] Examples of one-pot synthesis (OPS), where all enzymes are combined in a single reaction vessel, are rare and often entail extended production periods, ranging from one to two days, with considerable variability in final yields.^[22] Furthermore, the production of non-natural nucleotide sugar derivatives predominantly relies on wild-type enzymes,

which lack optimal catalytic efficiency for these substrates. Consequently, substantial quantities of enzymes are required to facilitate efficient and time-effective production processes.^[34] As a result, there is a growing demand for a dependable supply of azido-based derivatives of nucleotide sugars.

In this work, we aimed to establish a robust biocatalytic one-pot synthesis process for producing UDP-6-azido-GalNAc (Figure 1) at a gram scale, followed by the subsequent purification to obtain a pure product. However, only the fully acetylated precursor compound of 6-azido-GalNAc has been previously documented in the literature.^[11] For the synthesis outlined in this work, the precursor underwent deacetylation to render it in a form conducive to the enzyme-driven synthesis of UDP-6-azido-GalNAc. This was achieved with the help of the enzymes *B/NahK* and *HsAGX1*, which have previously been applied for the synthesis of various azido nucleotide sugars^[17,22–23] and the multigram production of UDP-GlcNAc and UDP-GalNAc.^[20] Based on the kinetic analysis of the wild-type enzymes, we aimed to upscale the production from the mg scale to a gram scale. Furthermore, we comprehensively evaluate and describe the critical steps in establishing enzyme cascades for gram-scale production. We also highlight the limitations encountered during the subsequent purification of an unnatural nucleotide sugar.

Results and Discussion

Enzyme Kinetics

Testing the kinetics of *B/NahK* and *HsAGX1* for the unnatural substrates 6-azido-GalNAc and 6-azido-GalNAc-1-P revealed a significantly lower substrate affinity than their natural substrates. However, due to the poor solubility of 6-azido-GalNAc and 6-azido-GalNAc-1-P, a kinetic determination of the V_{\max} and K_m values for *B/NahK* and *HsAGX1* was challenging.

The kinetic curves (Figure S3 and S6) revealed no saturation at concentrations of 20 mM 6-azido-GalNAc (*B/NahK*) and 10 mM 6-azido-GalNAc-1-P (*HsAGX1*). Consequently, the calculated V_{\max} values are considered apparent, as they do not reflect a fully saturated enzyme reaction, and we estimate the actual values to be lower. An apparent low V_{\max} accompanied this for both enzymes, 328 mU/mg for *B/NahK* (Figure S3) and 622 mU/mg for *HsAGX1* (Figure S6). Compared to the literature, the calculated specific activity of *B/NahK* for 6-azido-GalNAc was about a third of that for the natural substrate GalNAc.^[35] It was further assessed that *B/NahK* has activity towards UTP as a

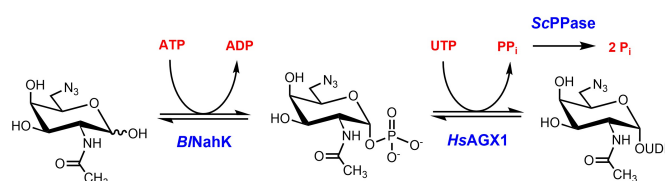


Figure 1. One-pot synthesis of UDP-6-azido-GalNAc with *B/NahK*, *HsAGX1*, and pyrophosphatase from *Saccharomyces cerevisiae* (*ScPPase*).

primary phosphate donor (Figure S7). Here, *B/NahK* showed a K_m of 1.9 mM for UTP and a maximal specific activity of 112 mU/mg. However, the kinetic of *B/NahK* also reveals that the poor affinity of UTP of the enzyme will only minorly affect the conversion within the synthesis cascade. *HsAGX1* showed an even lower activity with 6-azido-GalNAc-1-P, which was only a thirtieth of the reported activity for GalNAc-1-P.^[20] For the calculation of the K_m , a fully saturated kinetic curve is mandatory. We, therefore, calculated apparent K_m values for *B/NahK* and *HsAGX1*, which were 75 mM (*B/NahK*) and 15.7 mM (*HsAGX1*). When compared to the K_m values of the natural substrates (GlcNAc for *B/NahK* and GalNAc-1-P for *HsAGX1*), the enzymes display approximately 1.000 times (*B/NahK*) and 40 times (*HsAGX1*) higher K_m values.^[35–36] This mirrors the poor affinity of both enzymes to the used derivatized sugar and sugar-1-P. Furthermore, ATP substrate kinetics for *B/NahK* showed inhibition by ATP concentrations exceeding 10 mM with a calculated K_{i5} of 6.0 mM (Figure S4). However, considering the enzyme activity of *B/NahK* up to 10 mM ATP (Figure S5), a K_m of 0.26 mM was calculated, which is in the range of the reported K_m for ATP ($K_m=0.1$ mM).^[37] We also assessed an inhibition of *HsAGX1* by ADP. The specific activity decreased continuously with an increasing level of ADP, down to 24% residual activity at 15 mM ADP (Figure S8). The observed inhibition of *HsAGX1* by ADP (> 5 mM) and *B/NahK* by ATP (> 5 mM) is relevant for the enzyme cascade when high substrate concentrations in a one-pot synthesis are considered. 50 mM 6-azido-GalNAc and 50 mM ATP were almost not converted over 48 h by *B/NahK*, indicated by the very low ADP concentration determined by CE analysis (Figure S10). We concluded that

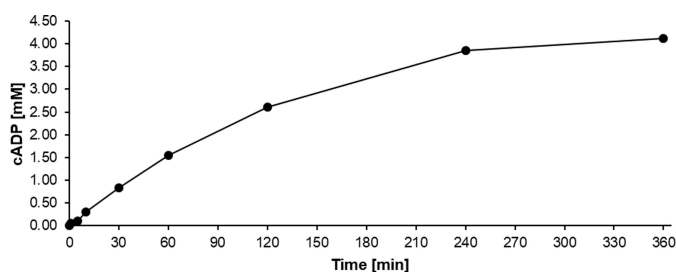


Figure 2. Synthesis of 6-azido-GalNAc-1-P by *B/NahK*. The reaction contained 5 mM 6-azido-GalNAc, 5 mM ATP, 50 mM Tris/HCl pH 8, 5 mM $MgCl_2$, 1.2 mg/mL *B/NahK* (394 mU/mL) and was done in a 50 mM Tris/HCl buffer pH 8.

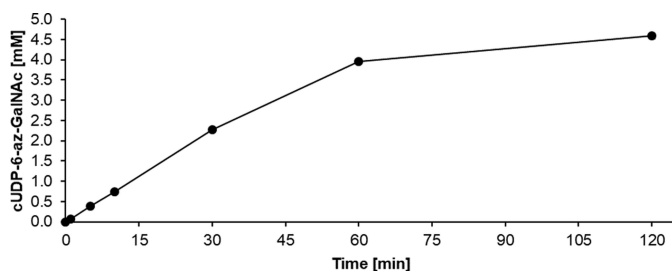


Figure 3. Conversion of 6-azido-GalNAc-1-P to UDP-6-azido-GalNAc by *HsAGX1*. The reaction contained 0.5 mg/mL *HsAGX1* (311 mU/mL), 2 U/mL ScPPase, 5 mM 6-azido-GalNAc-1-P, 5 mM UTP, 10 mM $MgCl_2$ and was performed in a 50 mM Tris/HCl buffer pH 8.

concentrations of 50 mM 6-azido-GalNAc and ATP are not applicable to the OPS cascade, as the *B/NahK* will be severely inhibited by ATP. Therefore, for the gram synthesis of UDP-6-azido-GalNAc substrate concentrations were defined to minimize *B/NahK* inhibition. The synthesis of 6-azido-GalNAc-1-P with *B/NahK* took significantly longer than the subsequent conversion of 6-azido-GalNAc-1-P with *HsAGX1*. It became evident that with 394 mU/mL (1.2 mg/mL) of *B/NahK*, a maximum conversion of 82% (4.12 mM) for a reaction with 5 mM 6-azido-GalNAc was achieved within 6 h (Figure 2). Interestingly, *HsAGX1*, despite its very low affinity for 6-azido-GalNAc-1-P, showed a significantly better conversion with 4.6 mM after 2 h (Figure 3).

Based on the results of the synthesis efficiency of each enzyme for the respective substrates (ATP and 6-azido-GalNAc for *B/NahK* and UTP and 6-azido-GalNAc-1-P for *HsAGX1*), we compared a one-pot and two-step synthesis (Figure S11). In the two-step synthesis, 6-azido-GalNAc-1-P was first synthesized by *B/NahK* overnight at RT (step 1), followed by removing the enzyme by filtration. *HsAGX1* and ScPPase were then added to the filtrate, with the reaction performed for 22 h (step 2). In the one-pot synthesis (OPS), both enzymes were combined with a 1.3-fold excess of *B/NahK* (Figure S11). For both approaches, the conversion of the substrates was determined after 6 h and 22 h. Here, the OPS achieved a conversion of 58% 6-azido-GalNAc within 6 h with a STY of $0.3 \text{ g}^* \text{L}^{-1} \text{ h}^{-1}$, which was further improved to a conversion of 93% 6-azido-GalNAc by extending the production time to 22 h. Conversely, the two-step synthesis only converted 26% 6-azido-GalNAc with a STY of $0.14 \text{ g}^* \text{L}^{-1} \text{ h}^{-1}$ within the first 6 h (Figure S11). Extending the synthesis to 22 h yielded a conversion of 54%, displaying only a minor improvement in the conversion efficiency.

Previous studies described the chemoenzymatic synthesis of UDP-6-azido-GalNAc in two steps. 6-azido-GalNAc-1-P was first synthesized by *B/NahK* with a 42% yield after 19 h, purified,^[38] and then converted by *HsAGX1* to a 61% yield after 6 h.^[22] In the same study, *HsAGX1* was compared to a bacterial GlmU, but the bacterial enzyme was significantly less effective than the human one. The low yield and poor STY of the two-step synthesis showcased the ineffective conversion of the substrates by splitting the single synthesis steps and supports using the synthesis in an OPS approach.

Optimization of the One-Pot Synthesis of UDP-6-Azido-GalNAc

A first described OPS to produce UDP-6-azido-GalNAc used a *B/NahK/HsAGX1* cascade for a synthesis over 12 h; however, no final yields were mentioned.^[39] Our previous study demonstrated *B/NahK/HsAGX1* as a fast enzyme cascade for the multi-scale production of UDP-GlcNAc and UDP-GalNAc by a rep.-batch process.^[20] To gain high productivity for synthesizing UDP-6-azido-GalNAc by rep.-batch, each batch reaction should give high product yields in a relatively short reaction time, resulting in a high space-time yield.

We concluded from the kinetic data that the low affinity of *B/NahK* for 6-azido-GalNAc requires significant quantities of

B/NahK compared to *HsAGX1* in a one-pot synthesis. Furthermore, substrate concentrations must be adapted to the kinetic data to gain maximum enzyme activity. A first one-pot synthesis with 2.5 mM and excess of *HsAGX1* showed only a moderate product yield of 78% with a low STY ($0.05 \text{ g}^* \text{L}^{-1} * \text{h}^{-1}$) after 24 h (Figure S12). We concluded that the concentrations of 6-azido-GalNAc and 6-azido-GalNAc-1-P remained significantly below the apparent K_m values of *B/NahK* and *HsAGX1*, substantially slowing down the enzyme reactions.

To further optimize the OPS, we aimed to reduce the reaction time by varying enzyme concentrations. *B/NahK* was raised to 4.7 mg/mL (1.5 U/mL), while the activity of *HsAGX1* was adjusted to 311 mU/mL (0.5 mg/mL) for OPS1 and 622 mU/mL (1 mg/mL) for OPS2. This is translated to a *B/NahK/HsAGX1* ratio of 4.8 (OPS1) and 2.4 (OPS2). Both OPS contained 10 mM 6-azido-GalNAc, 10 mM ATP, and 10 mM UTP and were incubated for 6 h. This ratio with an excess of *B/NahK* is critical to ensure the rapid conversion of 6-azido-GalNAc, and the limitation of the reaction is attributed by *HsAGX1*. As a result, both OPS showed good conversion of 6-azido-GalNAc with 90% (OPS1) and 89% (OPS2) within 6 h resulting in a STY of $1 \text{ g}^* \text{L}^{-1} * \text{h}^{-1}$ (OPS1) and $0.9 \text{ g}^* \text{L}^{-1} * \text{h}^{-1}$ (OPS2) (Table 1). Interestingly, the highest STY of $2 \text{ g}^* \text{L}^{-1} * \text{h}^{-1}$ was achieved after 2 h in OPS2, containing double the amount of *HsAGX1* compared to OPS1. In conclusion, comparing both OPS shows that an excess

of *B/NahK* improves the synthesis efficiency, and *HsAGX1* activity impacts the STY.

Further increase of the *HsAGX1* concentration at higher substrate concentrations resulted in increased STY with good product yields after 6 h (Table 2).

Two further one-pot syntheses were carried out with 2 mg/mL *HsAGX1* (1.2 U/mL) with 10 mM and 15 mM substrate, as well as an additional synthesis with 20 mM substrate and 1 mg/mL *HsAGX1* (622 mU/mL). After 6 h, all OPS resulted in at least 84% substrate conversion (Figure S13), with the highest STY values observed after 2 h with $2.0 \text{ g}^* \text{L}^{-1} * \text{h}^{-1}$ (10 mM), $3.3 \text{ g}^* \text{L}^{-1} * \text{h}^{-1}$ (15 mM), and $2.3 \text{ g}^* \text{L}^{-1} * \text{h}^{-1}$ (20 mM) (Table 2). The OPS with 15 mM and 20 mM performed comparably in terms of STY, with the OPS 20 mM still having a STY of $1.8 \text{ g}^* \text{L}^{-1} * \text{h}^{-1}$ after 6 h and OPS 15 mM $1.3 \text{ g}^* \text{L}^{-1} * \text{h}^{-1}$. In addition, OPS 20 mM had a higher final product concentration of 17.4 mM after 6 h than OPS 15 mM with 12.6 mM (Figure S14A). The challenge posed by a 6 h reaction time is that it limits a rep.-batch to only one reaction per working day under these conditions. However, when reducing the reaction time to 4 h, OPS 15 mM yielding 86% conversion and a STY of $2.0 \text{ g}^* \text{L}^{-1} * \text{h}^{-1}$ (Table 2) appears as practical. In our effort to optimize productivity with an OPS containing 30 mM 6-azido-GalNAc and 30 mM UTP, we observed that nearly no substrate was converted to 6-azido-GalNAc-1-P within 24 h. Subsequent analysis revealed minimal concentrations of 0.76 mM UDP-6-azido-GalNAc after 24 h (Figure S15), indicating a conversion yield of 2.5%. This observation suggests that the reaction is constrained not only by the poor enzyme activity but also by the substrate concentration.

In CE-analysis, it became evident that the purchased UTP contained UDP as detected at the start (t_{0h}) of the synthesis (Figure S14C), which gradually increased during the reaction, resulting in a reduction in the final product concentration of UDP-6-azido-GalNAc. We hypothesize that UTP is a secondary substrate for *B/NahK* as demonstrated by its activity towards UTP (Figure S5). It is most likely utilized when the kinase is not fully saturated with ATP. For instance, after 6 h, OPS 10 mM contained 1.4 mM (0.14 equiv.) UDP, while OPS 20 mM exhibited 2.6 mM UDP (0.13 equiv.), and OPS 15 mM showed a concentration of 2.4 mM UDP (0.16 equiv.). Furthermore, the dependence of the final product yield on the *HsAGX1* concentration becomes more evident by analyzing the UDP concentration in OPS 20 mM. The lower activity of *HsAGX1* (622 mU/mL) in the system led to a slower conversion of 6-azido-GalNAc-1-P into the nucleotide sugar, causing some of the UTP intended for monosaccharide phosphorylation to be utilized by *B/NahK*.

To compensate for the loss of UTP during the synthesis the UTP concentration was adjusted to 1.1 equiv., 1.2 equiv., and 1.4 equiv. to the substrates 6-azido-GalNAc and ATP. Since we saw in the previous OPS approach that the full conversion of all the available UTP was only achieved after 6 h, we further increased the activity of *B/NahK* and *HsAGX1* to 1.5 U/mL and 1.2 U/mL, respectively. Increasing UTP to 1.1 equiv. or 1.2 equiv. resulted in an 85% or 94% conversion of 6-azido-GalNAc in 4 h (Figure S16A). However, a further increase of the UTP did not improve the product yield. Interestingly, it was shown that

Table 1. OPS with 10 mM substrate (6-azido-GalNAc, ATP, and UTP) concentration for the UDP-6-azido-GalNAc synthesis in dependence on the *B/NahK/HsAGX1* ratio (OPS1: 4.8 and OPS2: 2.4).

	OPS1 ^[a]			OPS2 ^[b]		
	Conc. [mM]	Yield ^[c] [%]	STY [$\text{g}^* \text{L}^{-1} * \text{h}^{-1}$]	Conc. [mM]	Yield [%]	STY [$\text{g}^* \text{L}^{-1} * \text{h}^{-1}$]
2 h	4.5	45	1.5	6.2	62	2
4 h	8.3	83	1.3	8.3	83	1.4
6 h	9.0	90	1.0	8.9	89	0.9

[a]: 311 mU/mL *HsAGX1*. [b]: 622 mU/mL *HsAGX1*. [c]: Yields depicted from the initial 6-azido-GalNAc (main substrate) concentration.

Table 2. Performance of the one-pot synthesis of UDP-6-azido-GalNAc with 10 mM, 15 mM, and 20 mM substrate. The reaction was performed in 600 μL .

	Time	Conc. [mM]	Yield [%]	STY [$\text{g}^* \text{L}^{-1} * \text{h}^{-1}$]
OPS ^[a] 10 mM	2 h	6.3	63	2.0
	4 h	8.3	83	1.3
	6 h	8.6	86	0.9
OPS ^[a] 15 mM	2 h	10.4	69	3.3
	4 h	12.9	86	2.0
	6 h	12.6	84	1.3
OPS ^[b] 20 mM	2 h	7.2	36	2.3
	4 h	14.8	74	2.3
	6 h	17.4	87	1.8

[a]: Reaction contained 4.7 mg/mL *B/NahK* (1.5 U/mL) and 2 mg/mL (1.2 U/mL) *HsAGX1*. [b]: Reaction contained 2.3 mg/mL *B/NahK* (754 mU/mL) and 1 mg/mL (622 mU/mL) *HsAGX1*.

1.4 equiv. of UTP led to a less efficient conversion of 6-azido-GalNAC compared to the other reactions (Figure S16C). We assume that the high UTP concentration led to an inhibition of the system since after 4 h synthesis time, 3 mM of the used UTP was present as UDP (0.14 equiv.) and 12.1 mM (81 % yield) of UDP-6-azido-GalNAC was synthesized, leading to 5.8 mM of UTP which was not used in the reaction.

Therefore, we decided that an excess of 1.2 equiv. UTP would be most suitable for the rep.-batch production. In addition, further steps toward enzyme engineering are viable options for enhancing the OPS cascade. This was recently demonstrated for an E37S Galactokinase mutant with improved kinetic characteristics toward 6-azido-Gal in combination with a D113 V mutant of UDP-glucose pyrophosphorylase (GalU), both from *Streptococcus pneumoniae*. The development of a batch process for synthesizing UDP-6-azido-Gal with reasonable enzyme amounts in 24 h was demonstrated.^[40]

As a result of our findings from the single-batch OPS systems, we concluded that for the efficient production of 1 g UDP-6-azido-GalNAC in a rep.-batch process, a production time of 4 h per batch would be best since two single batches could be performed during one working day. We further assessed that *B/NahK* had to be added in high access to *HsAGX1* with 4.7 mg/mL (1.5 U/mL) *B/NahK* and 2 mg/mL (1.2 U/mL) *HsAGX1*. We further concluded that a substrate concentration of 15 mM of 6-azido-GalNAC and an excess of 1.2 equiv. UTP should lead to the best performance for a high-yield process. These parameters were then applied in a first small rep.-batch approach in a 5 mL scale.

Principles of Rep.-Batch Strategies

Since the 6-azido-GalNAC and 6-azido-GalNAC-1-P are unnatural substrates for *B/NahK* and *HsAGX1*, respectively, a proper production strategy had to be established to maximize the use of the enzyme and the production time. However, by storing the enzyme in the refrigerator overnight, the production potential of the OPS system is hardly reduced but stable over a more extended period since the overall incubation time is reduced. This will also decrease the enzyme destabilization and the associated effect of accelerated enzyme activity loss. On the other hand, the enzyme reaction could convert a higher substrate concentration overnight to enhance the final product yield. We suggest extending the published rep.-batch procedures by elongating the production overnight with a higher substrate concentration, which was most suitable for the rep.-batch. Furthermore, with a longer operation time at 37 °C, the enzyme concentration has to be adjusted since the potential of the reaction is reduced with every consecutive synthesis cycle.^[20,25]

Comparison of Repetitive Batch Synthesis of UDP-6-Azido-GalNAC in the 5 mL Scale

We produced UDP-6-azido-GalNAC in two separate repetitive batches (Figure 4). After 8 h (2 batch reactions with 15 mM substrate), RB1 was stored at 4 °C and RB2 was supplemented with a substrate solution containing 20 mM 6-azido-GalNAC, 20 mM ATP, and 24 mM UTP for an overnight production at 37 °C (Figure 4). Rep.-batch 1 (RB1) showed a higher overall productivity than RB2 (Table 3). After storage at 4 °C or overnight production at 37 °C, respectively, RB1 and RB2 showed comparable product concentrations of 14.9 mM and 12.8 mM in the first batch reaction. However, after the second batch (4 h–8 h), the product concentration in RB1 was 16.1 mM and higher than RB2 with 11.3 mM. During the overnight production (8 h–22 h) with 20 mM substrate, RB2 gained a product concentration of 15.6 mM, and both rep.-batches stayed steady in their productivity in the last two batches (22 h–30 h) with an average substrate concentration of 11.1 mM (RB1) and 10.0 mM (RB2).

In summary, RB1 showed higher productivity over the entire experiment, which means that storing the enzyme overnight at 4 °C supports the stability of the long-term synthesis more than a synthesis that is continued overnight. However, the long synthesis time of 4 h limits the overall productivity of the iterative approaches, as only a small amount of product can be formed in one working day. On the other hand, if the rep.-batch is used overnight to convert a higher substrate concentration, part of the synthesis time can be used for higher process productivity. Therefore, we conclude that synthesis with 15 mM

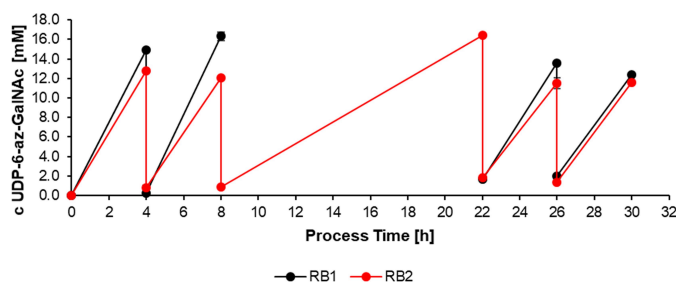


Figure 4. Performance of the repetitive batch synthesis of UDP-6-azido-GalNAC in a 5 mL scale. Two parallel repetitive batches (RB1 and RB2) were performed for 4 h each, with 15 mM 6-azido-GalNAC, 18 mM UTP, 15 mM ATP, 33 mM–44 mM MgCl₂, 4.7 mg/mL (1.5 U/mL) *B/NahK*, 2 mg/mL (1.2 U/mL) *HsAGX1*, 1 U/mL *ScPPase* and 100 mM Tris/HCl pH 8. After every synthesis step, the product solutions were separated by ultrafiltration, and fresh substrate was added. The enzymes of RB1 were stored at 4 °C overnight, and the synthesis continued the next day. The enzymes of RB2 were used for overnight production at 37 °C with 20 mM 6-azido-GalNAC, 20 mM ATP, and 24 mM UTP.

Table 3. Comparing rep-batches with overnight storage at 4 °C (RB1) and production overnight at 37 °C (RB2).

	Enzyme [mg]	Conc. ^[a] [mM]	Yield ^[a] [%]	Product [mg]	TTN [g _p /g _e]	Av. STY ^[a] [g*L ⁻¹ h ⁻¹]
RB1	33.5	13.4	89.3	118	3.5	2.1
RB2	33.5	11.3	75.2	132	3.9	1.6

[a]: Calculation displays the median value.

substrate and an overnight production with 20 mM substrate is the most appropriate approach. Both rep-batch strategies showed a stable production efficiency over several batches. However, the efficiency is reduced after three to four batches, as demonstrated for former repetitive batches.^[20,25] Therefore, adding small amounts of the enzyme after 3–4 batches is recommended to keep the production stable over a longer period.

Gram-Scale Production of UDP-6-Azido-GalNAc

The overnight production principle was chosen for the gram-scale production of UDP-6-azido-GalNAc, and the optimized process parameters were used. Three parallel batches (RB) with 20 mL each were run with five batch repetitions over 30 h. Four repetitive batches were performed with 15 mM 6-azido-GalNAc, 15 mM ATP, and 18 mM UTP for 4 h and one overnight batch with 20 mM 6-azido-GalNAc, 20 mM ATP, and 24 mM UTP (Figure 5). RB1 and RB3 showed almost complete conversion after every production cycle, averaging 97% for both batches. RB2 showed a lower substrate conversion, with an average yield of 77% (Table 4). The addition of 20% enzyme (18.8 mg *B/NahK*, 2.4 mg *HsAGX1*, and 0.02 mg *ScPPase*) after the overnight batch did not significantly impact the cascade (Figure 5).

RB1-3 produced between 662 mg, 600 mg, and 644 mg UDP-6-azido-GalNAc, resulting in an overall product amount of 1.9 g in 30 h (Table 4 and Table S2). In addition, satisfactory STYs ranging between $1.7 \text{ g}^* \text{L}^{-1} \text{ h}^{-1}$ and $2.2 \text{ g}^* \text{L}^{-1} \text{ h}^{-1}$ for the

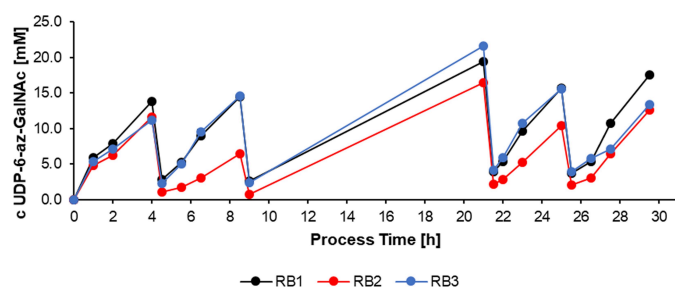


Figure 5. Rep-batch synthesis of UDP-6-azido-GalNAc. Batches 1, 2, 4, and 5 contained 15 mM 6-azido-GalNAc, 15 mM ATP, 18 mM UTP, 33 mM MgCl_2 and were performed in 100 mM Tris/HCl buffer pH 8 for 4 h each. The overnight production (batch 3) was done with 20 mM 6-azido-GalNAc, 20 mM ATP, 24 mM UTP, 44 mM MgCl_2 in 100 mM Tris/HCl. Each parallel batch contained 4.7 mg/mL (1.5 U/mL) *B/NahK*, 2 mg/mL (1.2 U/mL) *HsAGX1* and 1 U/mL *ScPPase*. At the beginning of batch 4, 18.8 mg *B/NahK*, 2.4 mg *HsAGX1*, and 0.02 mg *ScPPase* were added to each parallel batch. Each batch was made in a 20 mL scale.

syntheses over 4 h were obtained. For the production of 1.9 g product, a total of 405.96 mg enzymes was used (Table S3), translated into a total of 135.25 mg enzymes for every single batch. This was connected to a limitation of the process since the centrifugal concentrator clogged after every second batch due to the high enzyme concentration. This means that those concentrators are not suited for a large-scale process. However, examining the product growth (Figure S17) demonstrated that the rep-batch is not at the end of productivity even after five consecutive cycles (for each rep.-batch) and suggests that the process will remain stable for longer. The production rate of all rep-batches over the production period of 30 h was similar, with 0.022 g/h for RB1, 0.020 g/h for RB2, and 0.021 g/h for RB3 (Table 4). The poor affinity of the enzymes for the substrates 6-azido-GalNAc and 6-azido-GalNAc-1-P caused the low TTNs between 4.4 and 4.9 g_p/g_E at the end of the production period (Table 4). If the repetitive batch is compared with a single-batch synthesis, it becomes apparent that the enzymatic production of a high-value product such as UDP-6-azido-GalNAc is primarily limited by the high amounts of enzyme.

Therefore, we compared our process with a chemical synthesis of 12 g of UDP-6-azido-GalNAc^[11] to include the additional effort of enzyme purification in production. The chemical synthesis of UDP-6-azido-GalNAc takes around 7 steps and involves large amounts of starting materials. The process described uses firstly Ac_3 -6-azido-GalNAc, which is converted of the C1 phosphorylated sugar 6-azido-GalNAc-1-P (26% yield). In parallel, UMP imidazole ester is synthesized from UMP and subsequently coupled to the sugar-1-phosphate. The coupling of 6-azido-GalNAc-1-P and UMP imidazole ester to UDP-6-azido-GalNAc results in the formation of UDP-6-azido-GalNAc, yielding a final yield of 53%.^[11]

A significantly better conversion (> 90%) is achieved in enzymatic syntheses due to the high selectivity of the enzymes. In addition, a one-pot enzymatic synthesis eliminates the purification of product intermediates, which are time- and energy-consuming.

Furthermore, two steps for synthesizing the nucleotide sugar are required by conducting the synthesis by a one-pot synthesis. Nevertheless, we demonstrated that the repeated use of the enzymes can significantly reduce the need for repeated purification of enzymes.

	Yield ^[a] [%]	Concentration [mM]	Product amount [mg]	TTN [g_p/g_E]	STY ^[b] [$\text{g}^* \text{L}^{-1} \text{ h}^{-1}$]	Production rate [g/h]
RB1	97	16	662	4.9	2.4	0.022
RB2	77	12	600	4.4	1.7	0.020
RB3	97	15	644	4.8	2.2	0.021

[a]: Calculation displays the median value. [b]: Calculation displays the median productivity for a 4 h batch.

Purification of UDP-6-Azido-GalNAc

Before the product purification, a pool of all rep.-batches (5 mL and 20 mL), as well as from single batch experiments in the 5 mL scale (data not shown), were pooled into a single product solution to gain a maximum quantity of the nucleotide sugar. The quantity of the product in the solution was determined by single capillary electrophoresis, yielding 2.6 g (4.11 mmol). The solution was incubated with alkaline phosphatase (AP) for 48 h at 37 °C before the purification, and the dephosphorylation of the nucleotides was monitored by single capillary electrophoresis. AP was removed from the product solution after 48 h using cross-flow filtration (Figure S18). While the nucleotide reduction with alkaline phosphatase (AP), various peaks corresponding to nucleoside bases were identified. However, following an incubation period of 21 h to 48 h, the single capillary measurement revealed additional peaks that could not be attributed to any specific compound. The peaks were further analyzed by UPLC-MS (Figure S19 to S23), but we could not define the unknown compounds further.

The following purification of UDP-6-azido-GalNAc in > 2 g scale was performed with a standard in-house purification protocol. This consisted of a combination of an initial anion exchange chromatography followed by repeated desalting with reversed-phase chromatography. Remaining cations were exchanged to the physiologically acceptable sodium salt using cation exchange chromatography. With minor changes in the chromatographic stationary phases and infrastructure, this process is expected to be scalable up to ~100 g of UDP-6-azido-GalNAc or related nucleotide sugars.

With the preparation of the product solution and the purification of the nucleotide sugar, we purified 6-azido-GalNAc with a recovery of 81 % (Table 5).

Analysis of the Product UDP-6-Azido-GalNAc

After lyophilization, the product UDP-6-azido-GalNAc (2.1 g sodium salt, 3.32 mmol) was obtained as a white solid. The product was characterized by UPLC-MS (Figure S19–S23), ¹H-NMR (Figure S24), and ³¹P-NMR (Figure S25). ¹H-NMR (400 MHz, D₂O) δ (ppm): 7.97 (d, *J*=8.1 Hz, 1H), 5.99 (s, 1H), 5.97 (d, *J*=4.1 Hz, 1H), 5.54 (dd, *J*=7.3, 3.4 Hz, 1H), 4.46–4.34 (m, 2H), 4.33–4.16 (m, 5H), 4.07–3.93 (m, 2H), 3.60 (dd, *J*=12.8, 7.3 Hz, 1H), 3.50 (dd, *J*=12.8, 6.1 Hz, 1H), 2.09 (s, 3H). ³¹P-NMR (162 MHz, D₂O) δ (ppm): –11.24 (d, *J*=21.0 Hz), –13.0 (d, *J*=20.8 Hz). LC-MS (ESI-Neg) calculated for C₁₇H₂₅N₆O₁₆P₂[–] (M–H) 631.08, found

631.26. HPLC-UV purity of the product (254 nm) was 99.9%. On IR the azido peak of UDP-6-azido-GalNAc was clearly visible at ~2100 cm^{–1} (Figure S26).

Conclusions

In conclusion, our work has successfully achieved the enzymatic production of the unnatural sugar UDP-6-azido-GalNAc at the gram scale, showcasing the robustness of the enzyme cascade *B/NahK/HsAGX1* with satisfactory product yields. Notably, this process stands out for its simplicity and eco-friendliness, as it generates minimal toxic waste, thus facilitating the purification of the final product. Moreover, we can significantly reduce the reaction time in a batch synthesis to just 4 h by employing large quantities of enzymes. However, it is important to acknowledge that while our methodology has demonstrated its effectiveness at the lab scale, there remain considerable challenges in scaling it up to meet industrial demands. The higher enzyme requirement for this process compared to the production from a natural substrate is a noteworthy drawback. This challenge can potentially be mitigated through efforts to enhance enzyme production efficiency, enzyme engineering, or process engineering strategies, such as enzyme immobilization. In addition, by improving the enzymes through protein engineering, variants of *B/NahK* and *HsAGX1* with a better affinity for the substrate 6-azido-GalNAc could reduce the enzyme demand and possibly enable an increased number of batches per day. Despite the high amount of required biocatalysts, it is still possible to scale up the rep.-batch process further and carry it out on a larger scale in the L-scale. Furthermore, the rep.-batch production demonstrated that the system continued to operate steadily after 30 h, indicating the potential for further batches. Starting from 6-azido-GalNAc, we indeed see the potential to produce UDP-6-azido-GalNAc on a > 10 g scale using an enzymatic method while remaining within an industrially relevant range.

The proposed production strategies can be utilized to increase outcomes because they each have benefits and limitations. Larger filtration devices can handle larger volumes and product purification methods must be adapted to handle large product volumes.

Experimental Section

Cloning and Enzyme Production

Genes and vectors for the enzymes *B/NahK* and *HsAGX1* were provided in a pET22(b) vector (BioCat GmbH, GER) with C-terminal His₆-tag (Table S1). All enzymes were used and purified as described in our previous studies.^[20,41–44] The enzymes *HsAGX1* and *B/NahK* were produced in *Escherichia coli* BL21(DE3) Gold in shake flasks (up to 200 mL scale), starting from a preculture. Cells were harvested and resuspended in phosphate buffer (50 mM, pH 7.4, and 50 mM imidazole). The cells were lysed by sonication. The cell-free extract was then purified by immobilized metal affinity chromatography (IMAC) and eluted in a 50 mM phosphate buffer pH 7.4 containing 500 mM imidazole. Centrifugal concentrators (Amicon®, Germany)

Table 5. Purification efficiency of 6-azido-GalNAc.

Step	UDP-6-azido-GalNAc [mmol]	Recovery [%]
Product pool	4.11	100
Nucleotide dephosphorylation and filtration	3.95	96
Purification	3.32	81

were used to exchange the elution buffer with the storage buffer (50 mM Tris/HCl pH 8). Afterward, the purity of the elution was analyzed by SDS-PAGE (Figure S1).

Synthesis of 6-Azido-GalNAc

For the enzymatic synthesis of UDP-6-azido-GalNAc, 6-azido-GalNAc was provided from Ac₃-6-azido-GalNAc as described^[11] and deacetylated to be utilized for the synthesis (Figure S6). This results in 2 g of 6-azido-GalNAc.

MP-CE Analysis

Multiplexed capillary electrophoresis (MP-CE) is a high-performance analytic device that allows the simultaneous separation and analysis of samples in up to 96 capillaries. We optimized the MP-CE in our previous studies to separate adenine, uridine, and guanidine-based molecules such as nucleotides or nucleotide sugars in a cePRO 9600™ MP-CE system (Advanced Analytical Technologies, USA).^[42,45] The nucleoside di- and triphosphates of adenine and uridine and the nucleotide sugar UDP-6-azido-GalNAc were separated in fused silica capillaries with a separation length of 55 cm (total length 80 cm) and an inner diameter of 50 μm. The separation was performed in a 50 mM NH₄-acetate buffer (C. Roth; Germany), pH 9.2, including 1 mM EDTA (C. Roth; Germany) in an electric field force of 8 kV. Samples were injected by applying a vacuum for 5 s. The nucleotides and the nucleotide part of the nucleotide-sugar were detected at 254 nm with a UV-Vis detector. In addition, 1 mM of *para*-aminobenzoic acid (PABA; Sigma Aldrich; USA) and 4-aminophthalic acid (PAPA; Sigma Aldrich; USA) were used as internal standards.

Single Capillary Electrophoresis Analysis

Single capillary analysis was done with an Agilent 7100 capillary electrophoresis system (Agilent Technologies, USA) and a fused silica capillary (56 cm length; 50 μm id). Analytic measurements were done with a buffered solution containing 50 mM NH₄-Ac (C. Roth; Germany), 1 mM EDTA (C. Roth; Germany), pH 9.2. Analysis during the product preparation was performed with a buffered solution containing 48 mM boric acid (C. Roth; Germany) and 37.5 mM sodium tetraborate (Sigma Aldrich; USA) at pH 8.9. Nucleotides were detected by a UV-Vis detector at 254 nm for adenine bases and 262 nm for uridine bases. 1 mM of *para*-aminobenzoic acid (PABA; Sigma Aldrich; USA) was used as an internal standard.

UPLC-MS, ¹H- and ³¹P-NMR and IR Analyses

UPLC-MS analysis was carried out on Waters Acquity UPLC equipped with a diode array UV detector, an SQD ESI MS detector and a Waters Acquity BEH C18 1.7 μm column (PN 186002353). The injected sample was eluted with a gradient of a 50 mM Et₃N/HOAc buffer (pH 6.9) (A) and MeCN (B). The following gradient program was used: t = 0 min (100% A), t = 0.2 min (100% A), t = 12 min (95% A, 5% B), t = 13.5 min (80% A, 20% B), t = 14 min (100% A), t = 16 min (100% A) at a flow rate of 0.45 mL/min and a column temperature of 40 °C. NMR spectra were recorded on Bruker Biospin 400 MHz spectrometer. Samples were prepared in the indicated solvent. IR measurement was done on a PerkinElmer Spectrum Two (PerkinElmer, USA) with uATR accessory. The spectra were recorded over the range 4000–450 cm⁻¹ using a resolution of 4 cm⁻¹ and 16 scans.

Activity assays

The activities of *B/NahK* and *HsAGX1* were tested in 600 μL using 2.5 mM ATP and 2.5 mM 6-azido-GalNAc (*B/NahK*) or 2.5 mM 6-azido-GalNAc-1-P and 2.5 mM (*HsAGX1*). 1.2 mg/mL (*B/NahK*) or 0.5 mg/mL (*HsAGX1*) were added to each respective reaction. The reactions, containing *HsAGX1* were also supplemented with 1 U/mL ScPPase. All reactions were conducted for 2–6 h until the reactions showed a 10% conversion of the respective substrates and the specific activity was calculated accordingly (eq. 1.1).

$$a_s = \frac{\Delta[P]}{\Delta t} * \frac{V_R}{V_E} * F \quad (1.1)$$

a_s Specific activity (U/mg; μmol*min⁻¹ mg⁻¹),

$\Delta[P]$ Change of product concentration [mM],

Δt Time until 10% of the substrates are converted [min],

V_R Volume of the reaction [mL],

V_E Volume of enzyme added [mL],

F Dilution of enzyme prior to the reaction [–].

The reactions were stopped by adding 60 μL of the reaction solution to 60 μL stop-solution, containing 2 mM PABA, 14 mM SDS and 5 mM PAPA.

Kinetic Assays

All enzyme assays before the scale-up were done in 600 μL approaches in 1.5 mL reaction vessels at 37 °C for *HsAGX1* and *B/NahK*. All reactions were stopped with a solution containing 14 mM SDS, 2 mM PABA, and 2 mM PAPA and analyzed by MP-CE. The assays were done discontinuously at time points between 0 h and 6 h until the enzyme converted 10% of the substrate.

B/NahK assays were done with a gradient of 6-azido-GalNAc and ATP ranging from 0.5 mM to 20 mM for 6-azido-GalNAc (Synaffix; NL) and ATP (Carbosynth, GB), respectively. For the respective kinetic for ATP or 6-azido-GalNAc, the concentration of the other substrate was kept constant at 5 mM. Furthermore, all assays contained 1.2 mg/mL *B/NahK* and 20 mM MgCl₂ and were done in a 50 mM Tris/HCl buffer, pH 8. *HsAGX1* assays were only performed for 6-azido-GalNAc-1-P and with the same buffer conditions as *B/NahK*. Furthermore, the reaction contained a gradient of 6-azido-GalNAc-1-P (Synaffix; NL) reaching from 0.5 mM to 10 mM, 5 mM UTP (Carbosynth, GB), 10 mM MgCl₂, 0.5 mg/mL *HsAGX1* and 0.7 U/mL inorganic pyrophosphatase from *S. cerevisiae* (Roche, CH). Kinetic assays for the synthesis of GlcNac-1-P from GlcNac and UTP by *B/NahK* were done using 1–15 mM UTP, 2.5 mM GlcNac, 0.785 mg/mL *B/NahK*, 15 mM MgCl₂, and was done in a 100 mM Tris/HCl buffer pH 7.

The kinetics were calculated using the formula for the Michaelis-Menten equation (eq. 1.2). Regression for the kinetic parameters was made utilizing Sigmaplot 14.0 (Systat Software; Germany) for single substrate binding.

$$v_0 = \frac{v_{max} * [S]}{K_m + [S]} \quad (1.2)$$

Process Limitation Assays

To maximize the product yield for the synthesis of UDP-6-azido-GalNAc, a simple assay was constructed to first test the ability of *B/NahK* to catalyze the conversion of 6-azido-GalNAc at high substrate concentration. However, the substrate 6-azido-GalNAc was not soluble in the buffer at concentrations exceeding 100 mM. Therefore, we tested 50 mM 6-azido-GalNAc as the highest substrate concentration.

The reported activities are derived from the kinetic measurements for 6-azido-GalNAc (*B/NahK*) and (*HsAGX1*). The phosphorylation of excess 6-azido-GalNAc was tested in a 1 mL experiment with 50 mM 6-azido-GalNAc, 50 mM ATP, 50 mM $MgCl_2$, and 1.4 mg/mL *B/NahK* (16.6 mU/mL) in 50 mM Tris/HCl, pH 8 for 48 h at RT. The reaction was stopped with 14 mM SDS after 0 h, 24 h, and 48 h.

Furthermore, the two-step synthesis revealed that *HsAGX1* was not able to effectively convert 6-azido-GalNAc-1-P, which was previously prepared by *B/NahK* and contained also ADP. Since the kinetic analysis did not show any substrate inhibition by 6-azido-GalNAc-1-P, we assumed that *HsAGX1* is probably cross-inhibited by ADP. The effect of ADP on UDP-sugar synthesis by *HsAGX1* was tested with increasing concentrations of ADP starting from 0 mM to 15 mM, 5 mM UTP (Carbosynth; GB), 5 mM 6-azido-GalNAc-1-P (Synaffix; NL), 20 mM $MgCl_2$, 0.5 mg/mL *HsAGX1* and 0.6 U/mL ScPPase in 50 mM Tris/HCl, pH 8. All samples were analyzed by single-capillary electrophoresis. For both enzymes, the relative specific activity was calculated according to the procedure described in the kinetic section.

To further test limitations of *B/NahK* and *HsAGX1* by ATP and ADP, respectively, OPS was conducted with 30 mM 6-azido-GalNAc (Synaffix, NL), 30 mM ATP, 30 mM UTP, 60 mM $MgCl_2$, and 1 U/mL ScPPase (Roche; CH), 4.7 mg/mL (108 mU/mL) *B/NahK* and 2 mg/mL (764 mU/mL) *HsAGX1* were used in a 100 mM Tris/HCl buffer pH 8. The synthesis was conducted for 24 h at 37 °C on a 600 μ L scale. The reaction was stopped with a solution containing 14 mM SDS, 2 mM *para*-aminobenzoic acid (PABA; Sigma Aldrich; USA), and 2 mM 4-aminophthalic acid (PAPA; Sigma Aldrich; USA) and analyzed by MP-CE.

One Pot Synthesis (OPS)

First, OPS experiments were conducted for the proof of principle and then adjusted to the subsequent substrate and enzyme upscales. The stated activities are based on the calculated activities from the kinetic data for 6-azido-GalNAc (*B/NahK*) and 6-azido-GalNAc-1-P (*HsAGX1*). Initial experiments contained substrate concentrations of 2.5 mM 6-azido-GalNAc, 2.5 mM UTP, 2.5 mM ATP, 5 mM $MgCl_2$, and a 50 mM Tris/HCl buffer, pH 8. Synthetic OPS experiments with a scale of 20 mM 6-azido-GalNAc contained 24 mM UTP, 20 mM ATP, and 44 mM $MgCl_2$ in a 100 mM Tris/HCl buffer, pH 8. Concentrations of *B/NahK* and *HsAGX1* were varied from 1.2 mg/mL to 4.7 mg/mL *B/NahK* and 257 mg/mL to 2 mg/mL for *HsAGX1*, in addition to 0.6 U/mL to 2 U/mL of ScPPase (Roche, CH) were used. More details of the scale-up of the substrate concentrations are described in the particular result section. All reactions were done at 37 °C for 24 h and less, depending on the experimental setup. One pot synthesis was performed in a 600 μ L scale in a 1.5 mL reaction vessel and up-scaled to 5 mL before the rep-batch approaches, and the synthesis efficiencies were analyzed by MP-CE.

Two-Step Synthesis

A two-step synthesis of UDP-6-azido-GalNAc was done by separate syntheses of 6-azido-GalNAc-1-P and UDP-6-azido-GalNAc by *B/NahK* and *HsAGX1*, respectively. The stated activities are based on the calculated activities from the kinetic data for 6-azido-GalNAc (*B/NahK*) and 6-azido-GalNAc-1-P (*HsAGX1*). The sugar-phosphate was synthesized with 1.2 mg/mL *B/NahK*, 10 mM ATP, and 10 mM $MgCl_2$ in 50 mM Tris/HCl, pH 8, for 24 h at RT. Afterward, *B/NahK* was removed by ultrafiltration, using a centrifugal concentrator with 30 kDa MWCO (Vivaspin™ 20, Sartorius, Germany). The synthesis was analyzed by single-capillary electrophoresis, and the concentration of 6-azido-GalNAc-1-P was theoretically calculated by the concentration of detected ADP. UDP-6-azido-GalNAc was then synthesized with the filtrated solution containing 4.1 mM 6-azido-GalNAc-1-P, 0.25 mM AMP, 0.6 mM ATP, and 4.1 mM ADP with 0.5 mg/mL *HsAGX1*, 1.2 U/mL ScPPase (Roche, CH), 5 mM UTP and 10 mM $MgCl_2$ in 50 mM Tris/HCl, pH 8. The synthesis efficiency for UDP-6-azido-GalNAc was analyzed by MP-CE.

Rep-Batch Production of UDP-6-Azido-GalNAc

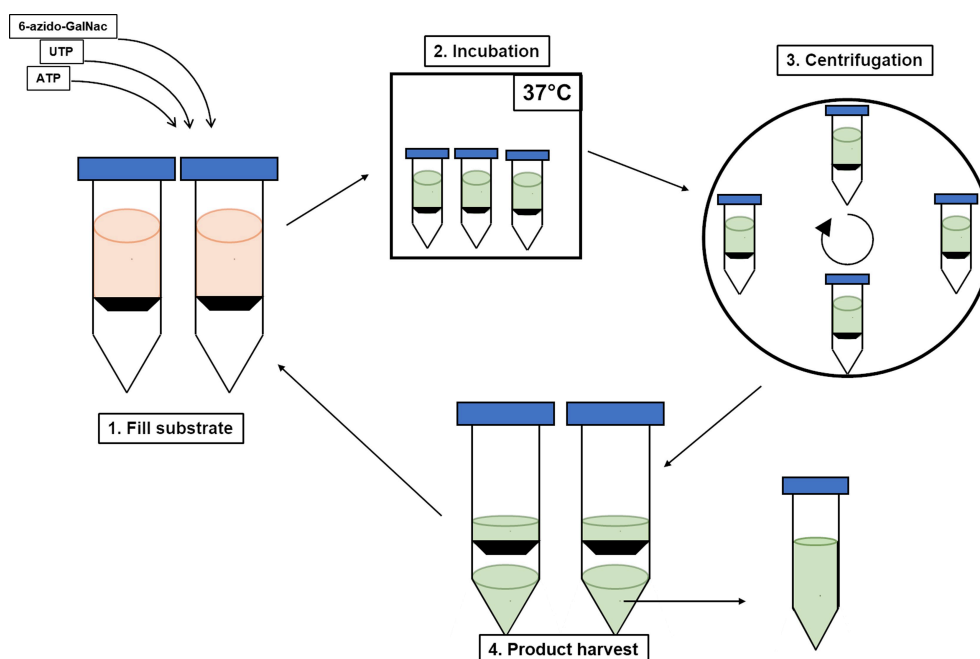
The rep-batch production (Scheme 1) was performed in two ways. Two parallel rep-batches in a 5 mL scale were conducted, while one rep-batch was continuously held at production and the other stored overnight at 4 °C. The 5 mL rep batches were done in four batches with a starting enzyme concentration of 4.7 mg/mL (1.5 U/mL) *B/NahK*, 2 mg/mL (1.2 U/mL) *HsAGX1*, and 1 U/mL ScPPase. Each batch was conducted for 4 h at 37 °C in a 20 mL ultracentrifugation tube (Vivaspin™ 20; Sartorius, Germany) with 15 mM 6-azido-GalNAc (Synaffix, NL), 15 mM ATP (Sigma Aldrich, USA), 18 mM UTP (Carbosynth, GB) and, 33 mM $MgCl_2$ in 100 mM Tris/HCl, pH 8. The over-night production was done with 20 mM 6-azido-GalNAc (Synaffix, NL), 20 mM ATP (Sigma Aldrich, USA), 24 mM UTP (Carbosynth, GB), 44 mM $MgCl_2$ in 100 mM Tris/HCl, pH 8. After every batch, the tube was centrifugated at 4000 rpm for 30 minutes at 4 °C until a remaining volume of 1 mL was reached, and the permeate was stored at -20 °C. After the centrifugation, 4 mL of new substrate was added to the solution.

The 20 mL scale rep-batch production was done in three parallel batches with a starting enzyme concentration of 4.7 mg/mL (1.5 U/mL) *B/NahK*, 2 mg/mL (1.2 U/mL) *HsAGX1*, and 1 U/mL ScPPase. The stated activities are based on the calculated activities from the kinetic data for 6-azido-GalNAc (*B/NahK*) and 6-azido-GalNAc-1-P (*HsAGX1*). Batch production throughout 4 h was conducted at 37 °C in a 20 mL ultracentrifugation tube (Vivaspin™ 20; Sartorius, Germany) with 15 mM 6-azido-GalNAc (Synaffix, NL), 15 mM ATP (Sigma Aldrich, USA), 18 mM UTP (Carbosynth, GB), and 33 mM $MgCl_2$ in 100 mM Tris/HCl, pH 8. The overnight production was done with 20 mM 6-azido-GalNAc (Synaffix, NL), 20 mM ATP (Sigma Aldrich, USA), 24 mM UTP (Carbosynth, GB), 44 mM $MgCl_2$ in 100 mM Tris/HCl, pH 8. After each batch, the tube was centrifugated at 4000 rpm for 30 min at 4 °C, and the permeate was stored at -20 °C.

All samples were treated with a stop solution containing 14 mM SDS, 2 mM *para*-aminobenzoic acid (PABA; Sigma Aldrich; USA), and 2 mM 4-aminophthalic acid (PAPA; Sigma Aldrich; USA) and measured by MP-CE.

Product Preparation for the Purification

The product solution was prepared for subsequent ion exchange (IEX) purification by digesting the remaining nucleotides ATP, ADP, AMP, UTP, UDP, and UMP by alkaline phosphatase (AP). The



Scheme 1. The general procedure of a rep.-batch production.

product solutions from each batch were pooled (280 mL) in a single vessel and adjusted to pH 8. Afterward, 6,000 U of alkaline phosphatase (AP, SERVA, Germany) was added and incubated at 37 °C with gentle shaking at 80 rpm for 48 h. The reaction was monitored after 0 h, 21 h, and 48 h. Each sample was prepared with 1 mM PABA and analyzed by single capillary electrophoresis using the previously described borate buffer protocol. To remove AP after 48 h, a cross-flow filtration membrane cassette (Vivaflow® 50 R; Sartorius; Germany) with 30 kDa MWCO was used. The AP-containing solution was filtered by cross-flow filtration to a residual volume of 5 mL, and the membrane was washed with 100 mL of ultrapure water to harvest residual product. A UDP-6-azido-GalNAc standard (Synaffix, NL) with a single CE analysis quantified product concentration in the filtrate. The standard contained 0.25–1.25 mM UDP-6-azido-GalNAc and 1 mM para-aminobenzoic acid (PABA; Sigma Aldrich; USA). The quantification was done with single capillary electrophoresis following the previously described borate protocol.

Purification of UDP-6-Azido-GalNAc

The UDP-6-azido-GalNAc raw mixture was filtered through 0.45 µm regenerated cellulose membranes and was diluted to 1.5 L with water, followed by passage over a column with immobilized AP (SERVA, Heidelberg, Germany) (50×35 mm; 40 kU) overnight at room temperature to degrade residual monophosphates. After this step, 5'-UMP and 5'-AMP were barely measurable in analytical HPLC. The HPLC system consisted of a L-7100 Intelligent pump, a L-7400 UV Detector, and a D-7500 Integrator (all Merck / Hitachi, Darmstadt, Germany). Stationary phase: YMC ODS-A 120-11, RP-18 (YMC, Dinslaken, Germany) 250×4 mm. Mobile phase: 8% (v/v) acetonitrile, 4 mM tributylammonium (TBA)-hydrogen sulfate buffer, 25 mM sodium dihydrogen phosphate buffer, pH 6.8; 1.0 mL/min; UV 262 nm.

For purification, the resulting product-containing raw mixture was diluted to 8.2 L and applied to a Q Sepharose™ Fast Flow anion exchange column (Cytiva, Munich, Germany) (45–165 µm;

380×50 mm), Cl⁻-form, previously regenerated with 2 M sodium chloride. Afterwards, the column was washed with water, followed by a gradient from 0–0.4 M triethylammonium bicarbonate (TEAB), pH~8, and UDP-6-azido-GalNAc was eluted with ~0.09 M TEAB →~0.15 M TEAB. After this step, the target compound was pure (99.50% HPLC). Product-containing fractions were desalted by repeated preparative reversed-phase medium-pressure liquid chromatography (MPLC). The product solution was applied to a Merck LiChrorep®RP-18 pre-column (Merck, Darmstadt, Germany) (40–63 µm; 80×35 mm) connected to a Merck LiChrorep®RP-18 column (15–25 µm; 445×50 mm) previously equilibrated with water. 100% water was used to remove the majority of TEAB-buffer, followed by elution of UDP-6-azido-GalNAc, TEA-salt (99.78% HPLC purity).

Final cation exchange to sodium was performed with a Toyopearl SP 650-M cation exchanger (Tosoh Bioscience, Griesheim, Germany) (40–90 µm; 380×50 mm), Na⁺-form. The product solution was filtered (0.45 µm reg. cellulose), diluted to 4 L, and passed over the cation exchange column. The column was then rinsed with ultrapure water until the eluate was free of UV absorption.

UDP-6-azido-GalNAc was carefully evaporated to dryness, dissolved in a small volume of ultrapure water, transferred to a glass tube, frozen at –70 °C for 2 h, and lyophilized. The final product yield was 2.1 g UDP-6-azido-GalNAc, sodium salt, purity: 99.96% by HPLC.

Formula (Free Acid): C₁₇H₂₆N₆O₁₆P₂ (MW 632.37 g/mol)

UV-Vis (water pH 7.0): λ_{max} 262 nm; ε 10000.

UV-spectra were recorded on a JASCO V-650 spectrometer JASCO, Pfungstadt, Germany) in phosphate buffered aqueous solution (pH 7).

ESI-MS pos. mode: *m/z* 633 (M+H)⁺, neg. mode: *m/z* 631 (M–H)[–]. Mass spectra were generated with a Bruker Esquire LC 6000 spectrometer (Bruker, Bremen, Germany) in the electrospray

ionization mass spectrometry (ESI-MS) mode with 50% water (v/v) /49.5% methanol (v/v)/0.5% NH₃ (v/v) (pH 9–10) as a matrix.

Acknowledgements

The authors thank Synaffix BV for their financial support. Open Access funding enabled and organized by Projekt DEAL.

Conflict of Interests

The authors declare no conflict of interest.

Data Availability Statement

The data that support the findings of this study are available in the supplementary material of this article.

Keywords: Repetitive Batch · Nucleotide sugars · Enzyme cascades · Azido-sugars

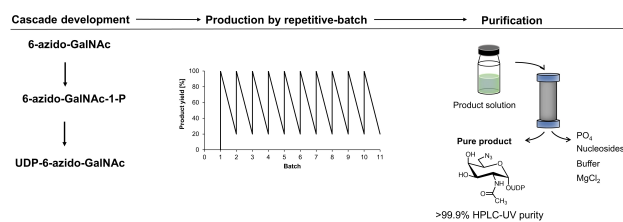
- [1] C. Bertozzi, *ACS Cent. Sci.* **2023**, *9*, 558–559.
- [2] N. J. Agard, J. M. Baskin, J. A. Prescher, A. Lo, C. R. Bertozzi, *ACS Chem. Biol.* **2006**, *1*, 644–648.
- [3] N. Nischan, J. J. Kohler, *Glycobiology* **2016**, *26*, 789–796.
- [4] X. Fan, Q. Song, D.-e. Sun, Y. Hao, J. Wang, C. Wang, X. Chen, *Nat. Chem. Biol.* **2022**, *18*, 625–633.
- [5] L. Shen, K. Cai, J. Yu, J. Cheng, *ACS Omega* **2020**, *5*, 14111–14115.
- [6] H. Möller, V. Böhrsch, J. Bentrop, J. Bender, S. Hinderlich, C. P. Hackenberger, *Angew. Chem. Int. Ed. Engl.* **2012**, *51*, 5986–5990.
- [7] E. Saxon, C. R. Bertozzi, *J. Sci.* **2000**, *287*, 2007–2010.
- [8] W. Lai-Xi, T. Xin, L. Chao, P. G. John, L. Tiezheng, *Annu. Rev. Biochem.* **2019**, *88*, 433–459.
- [9] K. Tsuchikama, Z. An, *Protein Cell* **2018**, *9*, 33–46.
- [10] X. Li, T. Fang, G.-J. Boons, *Angew. Chem. Int. Ed.* **2014**, *53*, 7179–7182.
- [11] M. A. Wijdeven, R. van Geel, J. H. Hoogenboom, J. M. M. Verkade, B. M. G. Janssen, I. Hurkmans, L. de Bever, S. S. van Berkel, F. L. van Delft, *mAbs* **2022**, *14*, 2078466.
- [12] R. van Geel, M. A. Wijdeven, R. Heesbeen, J. M. M. Verkade, A. A. Wasiel, S. S. van Berkel, F. L. van Delft, *Bioconjugate Chem.* **2015**, *26*, 2233–2242.
- [13] S. Mikkola, *Molecules* **2020**, *25*, 5755.
- [14] G. K. Wagner, T. Pesnot, R. A. Field, *Nat. Prod. Rep.* **2009**, *26*, 1172–1194.
- [15] M. Qiao, B. Li, Y. Ji, L. Lin, R. Linhardt, X. Zhang, *Crit. Rev. Biotechnol.* **2021**, *41*, 47–62.
- [16] J. G. Moffatt, H. G. Khorana, *J. Am. Chem. Soc.* **1958**, *80*, 3756–3761.
- [17] L. Cai, W. Guan, M. Kitaoka, J. Shen, C. Xia, W. Chen, P. G. Wang, *Chem. Commun.* **2009**, *19*, 2944–2946.
- [18] Z. A. Morrison, M. Nitz, *Carbohydr. Res.* **2020**, *495*, 108071.
- [19] Y. Li, H. Yu, Y. Chen, K. Lau, L. Cai, H. Cao, V. K. Tiwari, J. Qu, V. Thon, P. G. Wang, X. Chen, *Molecules* **2011**, *16*, 6396–6407.
- [20] T. Fischöder, C. Wahl, C. Zerhusen, L. Elling, *Biotechnol. J.* **2019**, *14*, 1800386.
- [21] H. Frohnmeyer, L. Elling, *Carbohydr. Res.* **2022**, *523*, 108727.
- [22] W. Guan, L. Cai, P. G. Wang, *Chem. J.* **2010**, *16*, 13343–13345.
- [23] Y. Chen, V. Thon, Y. Li, H. Yu, L. Ding, K. Lau, J. Qu, L. Hie, X. Chen, *Chem. Commun.* **2011**, *47*, 10815–10817.
- [24] T. Rexer, D. Laaf, J. Gottschalk, H. Frohnmeyer, E. Rapp, L. Elling, *Adv. Biochem. Eng. Biotechnol.* **2021**, *175*, 1–36.
- [25] H. Frohnmeyer, S. Rueben, L. Elling, *ChemCatChem* **2022**, *14*, e202200443.
- [26] T. F. T. Rexer, A. Schildbach, J. Klapproth, A. Schierhorn, R. Mahour, M. Pietzsch, E. Rapp, U. Reichl, *Biotechnol. Bioeng.* **2018**, *115*, 192–205.
- [27] H. Ohashi, C. Wahl, T. Ohashi, L. Elling, K. Fujiyama, *Adv. Synth. Catal.* **2017**, *359*, 4227–4234.
- [28] C. Wahl, M. Spiertz, L. Elling, *J. Biotechnol.* **2017**, *258*, 51–55.
- [29] K. Schmölzer, M. Lemmerer, A. Gutmann, B. Nidetzky, *Biotechnol. Bioeng.* **2017**, *114*, 924–928.
- [30] S. Ahmadipour, L. Beswick, G. J. Miller, *Carbohydr. Res.* **2018**, *469*, 38–47.
- [31] R. Mahour, J. Klapproth, T. F. T. Rexer, A. Schildbach, S. Klamt, M. Pietzsch, E. Rapp, U. Reichl, *J. Biotechnol.* **2018**, *283*, 120–129.
- [32] R. Mahour, J. W. Lee, P. Grimpe, S. Boecker, V. Grote, S. Klamt, A. Seidel-Morgenstern, T. F. T. Rexer, U. Reichl, *ChemBioChem* **2022**, *23*, e202100361.
- [33] S. Wang, J. Zhang, F. Wei, W. Li, L. Wen, *J. Am. Chem. Soc.* **2022**, *144*, 9980–9989.
- [34] Y. Guo, J. Fang, T. Li, X. Li, C. Ma, X. Wang, P. G. Wang, L. Li, *Carbohydr. Res.* **2015**, *411*, 1–5.
- [35] M. Nishimoto, M. Kitaoka, *Appl. Environ. Microbiol.* **2007**, *73*, 6444–6449.
- [36] A. Wang-Gillam, I. Pastuszak, A. D. Elbein, *J. Biol. Chem.* **1998**, *273*, 27055–27057.
- [37] M. Sato, T. Arakawa, Y. W. Nam, M. Nishimoto, M. Kitaoka, S. Fushinobu, *Biochim. Biophys. Acta* **2015**, *1854*, 333–340.
- [38] L. Cai, W. Y. Guan, W. J. Wang, W. Zhao, M. Kitaoka, J. Shen, C. O'Neil, P. G. Wang, *Bioorg. Med. Chem. Lett.* **2009**, *19*, 5433–5435.
- [39] L. Wen, M. R. Gadi, Y. Zheng, C. Gibbons, S. M. Kondengaden, J. Zhang, P. G. Wang, *ACS Catal.* **2018**, *8*, 7659–7666.
- [40] M. E. Ortiz-Soto, M. Baier, D. Brenner, M. Timm, J. Seibel, *J. Glycobiol.* **2023**, *33*, 651–660.
- [41] A. Eisele, H. Zaun, J. Kuballa, L. Elling, *ChemCatChem* **2018**, *10*, 2969–2981.
- [42] J. Gottschalk, H. Zaun, A. Eisele, J. Kuballa, L. Elling, *Int. J. Mol. Sci.* **2019**, *20*, 5664.
- [43] J. Gottschalk, L. Blaschke, M. Aßmann, J. Kuballa, L. Elling, *ChemCatChem* **2021**, *13*, 3074–3083.
- [44] J. Gottschalk, M. Aßmann, J. Kuballa, L. Elling, *ChemSusChem* **2022**, *15*, e202101071.
- [45] C. Wahl, D. Hirtz, L. Elling, *Biotechnol. J.* **2016**, *11*, 1298–1308.

Manuscript received: February 14, 2024

Revised manuscript received: March 27, 2024

Accepted manuscript online: April 24, 2024

Version of record online: ■■■, ■■■



This study offers an in-depth view of process development for the enzymatic synthesis of the unnatural nucleotide sugar UDP-6-azido-GalNAc. Through the implementation of an enzyme cascade comprising three different enzymes and utilizing the re-

petitive-batch procedure for nucleotide sugar production, followed by high-performance purification, we successfully generated 2.1 g of UDP-6-azido-GalNAc with an HPLC-UV purity grade of > 99.9%.

*H. Frohnmeyer, Dr. J. M. M. Verkade, M. Spiertz, Dr. A. Rentsch, N. Hoffmann, M. Sobota, Dr. F. Schwede, P. Tjeerdsma, Prof. Dr. L. Elling**

1 – 12

Process Development for the Enzymatic Gram-Scale Production of the Unnatural Nucleotide Sugar UDP-6-Azido-GalNAc

